Synthesis, spectral characterization, cyclic voltammety, molecular modeling and catalytic activity of sulfa-drug divalent metal complexes

Safaa N. Abdou[1], Abeer A. Faheim[1,2] and Abdel-Nasser M. A. Alaghaz[3,4]

[1]Chemistry Department, College of Education and Science (Khurma), Taif University, Al-khurma, Taif, Saudi Arabia
[2]Chemistry Department, Faculty of Science (Girl's), Al-Azhar University, P.O. Box 11754, Nasr-City, Cairo, Egypt
[3]Chemistry Department, Faculty of Science (Boy's), Al-Azhar University, P.O. Box 11754, Nasr-City, Cairo, Egypt (aalajhaz@hotmail.com)
[4]Chemistry Department, Faculty of Science, Jazan University, Jizan, Saudi Arabia

Abstract

Complexes of cobalt(II), nickel(II), copper(II), zinc(II) and Hafnium(II) of general composition $[M(L)_2(Cl)_2]$ have been synthesized [L = 4-(phenylphosphinylideneamino-N-thiazolyl benzene-sulfonamide]. The elemental analysis, molar conductance measurements, magnetic susceptibility measurements, mass, IR, UV, NMR, SEM, EDX, thermal and EPR spectral studies of the compounds led to the conclusion that the ligand acts as a bidentate manner. The molar conductance of the complexes in fresh solution of DMSO lies in the range of 7.46–9.13 Ω^{-1} cm^{2}mol^{-1} indicating their non-electrolytic behavior. On the basis of analytical and spectroscopic techniques, octahedral geometry of the complexes was proposed. The ligand acts as bidentate ligand, coordinated through sulfonamide oxygen and thiazole nitrogen atoms. The ligand field parameters were calculated for Co(II), Ni(II) and Cu(II) complexes and their values were found in the range reported for a octahedral structure. The catalytic activities of the divalent metal complexes have been studied in the oxidation of cyclohexane, using environmental friendly oxidant, hydrogen peroxide. Complex with rough surface has shown higher catalytic activity compared to the other complexes. The molecular parameters of the ligand and its Co(II) and Hf(II) complexes have been calculated.

Keywords: Schiff base; complexes; Spectroscopic; molecular parameters; SEM/EDX

Introduction

Currently available methods for the removal of phenol/phenolic compounds from wastewaters (chemical oxidation, reverse osmosis, adsorption and others) are expensive, have regeneration problems and may produce themselves wastewaters with a high environmental impact [1,2]. Particularly contaminating waste waters are those generated by textile and paper mill industries. These wastewaters include medium to low concentrations ofdyes or pigments. The degradation of dyes is one of the most important research fields in wastewater treatments. Researchers have recently focused on enzymatic treatments. Many peroxidases such as lignin peroxidase, manganese peroxidase, soybean peroxidase, horseradish peroxidase (HRP), laccase, polyphenol oxidases, microperoxidases and azoperoxidases have been used for the removal of dyes in industrial effluents [3–6]. One of the most studied substrates is phenol, which is frequently used as a simple model compound of more complex pollutants such as dyes, pigments and others. Among the most toxic phenolic compounds are the chloro– or nitro-substituted phenols. The secompounds are used as pesticides and anti–bacterials[7].Phenol is present in wastewaters discharged by resin manufacturing, petrochemical, oil-refining, paper mill, coking, and irons melting industries [8]. Phenol derivatives include anthraquinone dyes, an important group of dyes. Phenolic groups, besides being part of many dyes and pigments, are also the main moiety of lignin. Nowadays, high amounts of ligno-cellulosic wastes from paper and wood industries are generated, of which only 1–2%are reused. Therefore, their accumulation represents a serious environmental problem. Moreover, high-valuable products potentially obtainable from lignin degradation are misspent [9]. The enzymatic complex (Li-peroxidase, Mn-peroxidase and laccase) produced by white-rot fungi is able to degrade lignin up to mineralization. Hence, the application of well-known, commercially available and robust enzymes such as HRP is an attractive approach for lignin degradation. Recent studies on totally chlorine-free processes for pulping and bleaching involve the use of oxygen, ozone or hydrogen peroxide as oxidants, and enzymes or biomimetics as catalysts [10].There are three main research fields in the heterogeneous catalytic degradation of phenols: the catalytic wet-peroxide oxidation [11], the catalytic ozonation[12] and the catalytic wet oxidation 13]. The catalysts used in wet-peroxide oxidation include metal-exchanged zeolites, hydrotalcite-like compounds, metal-exchanged clays and resins. The catalysts used in catalytic wet oxidation are transition metal oxides and supported noble metals [14].

Thus, in this paper we synthesized a new tridentate Schiff base containing N_2O donor atoms and its cobalt(II), nickel(II), copper(II), zinc(II) hafnium(II) complexes. The HL ligand and its complexes were characterized by the FT-IR, ^{1}H NMR, ^{13}C NMR, mass, SEM, EDX, UV–Vis spectroscopy, elemental analysis, magnetic susceptibility, molar conductance and thermal analysis. The geometry of the complexes is characterized by means of spectral and magnetic measurements.

Experimental

Materials

All the chemicals and solvents used in this study were of AnalaR grade. The metal salts and the reagents used in this work were supplied from Aldrich and Fluka.

Analytical and physical measurements

The percentage of carbon, hydrogen, nitrogen and sulfur contents were analysed using Carlo Erba 1108 model elemental nalyser using sulphanilamide as a reference standard. The metal content presents in the complexes was estimated as given in the book [23]. Infrared spectra were recorded by using a 1% of the sample on KBr pellet with 16 scans and 2 cm^{-1} resolution in a Jasco FT-IR/4100 spectrophotometer equipped with ATR accessory in the range of 4000–400 cm^{-1}. The electronic spectra of the complexes in UV–Vis region were obtained in DMSO solutions using a Shimadzu UV-1601 spectrophotometer in the range of 200–800 nm. Magnetic susceptibility measurements were computed on a modified HertzSG8-5HJ model Gouy magnetic balance using $CuSO_4.5H_2O$ as the calibrant. Molar conductance of the complexes were studied in 10^{-3} M DMSO solution, using a deep vision model 601 digital direct reading deluxe conductivity meter at room temperature. The ^{1}H NMR spectrum of OIAC was investigated with a Bruker 300 Avance DRX 300 FT-NMR spectrometer in 1% HCl/D_2O solution using TMS as standard. ^{31}P NMR spectra were run, relative to external $H_3PO_4(85\%)$, with a varian FT-80 spectrometer at 36.5 MHz. Thermal studies (Thermo gravimetric (TG) analysis) were manipulated under a dynamic N_2 atmosphere in the 20–800 ºC range at a heating rate of 10 ºC min^{-1} on a Mettler Toledo star system. X-ray powder diffraction determinations were accomplished using an X-ray diffractometer ((XPERT PRO PANalytical, Netherland)) for phase identification. The patterns were run with Cu Ka radiation with a secondary monochromator (k = 0.1545 nm) at 40 kV and 30 mA. The surface morphology of chitosan, OIAC and the complexes were observed using a scanning electron microscope of model SEM-JSM 6390 at an accelerating voltage of 18 kV with a magnification range of 5 KX at liquid nitrogen temperature. Cyclic voltammograms were obtained on a CHI-600A electrochemical analyzer using a three electrode set-up comprising of a glassy carbon working, platinum wire auxiliary and a Ag/AgCl reference electrode under oxygen free conditions. A ferrocene/ferrocenium (1[+]) couple was used as an internal standard and $E_{1/2}$ of the ferrocene/ferrocenium (Fc/Fc[+]) couple under the experimental condition is found to be 470 mV. TBAP was used as asupporting electrolyte. Molar conductivity was measured by using an Elico digital conductivity bridge model CM-88 using freshly prepared solution of the complex in acetonitrile. The hydrolysis of 4–nitrophenylphosphate by the metal(II) complexes were studied in a 10^{-3}M dimethylformamide solution. Scanning electron microscopy (SEM) images were taken in Quanta FEG 250 equipment. The reaction was followed spectrophotometrically and the hydrolysis of 4-nitrophenylphosphate was monitored by following the UV–Vis absorbance change at 420nm (assigned to the 4-nitrophenolate anion) as a function of time. A plot of log $(A_\alpha/A_\alpha - A_t)$ versus time was made for all the complexes.

Isolation of ligand

Sulfathiazole [N_1-4-amino-thiazolylbenzenesulfonamide] (0.1 mol) in 100 ml cold dry benzene was added in small portions to a well stirred cold solution of dichlorophenylphosphine (0.l mol) in 100 ml cold dry benzene during half an hour at~15 ºC under dry conditions. After completion of the reaction (HCl gas ceased to evolve), the reaction mixture was filtered while hot and the solid obtained was washed several times with dry benzene, diethyl ether and dried in vacuo to give the corresponding 4-(phenylphosphinylideneamino-N-thiazolyl benzene-sulfonamide (HL) (Fig. 1). [$C_{15}H_{12}N_3O_2PS_2$]: yellow, yield; 86%, m.p.= 150-152ºC, Calculated C, 49.85; H, 3.35; N, 11.63; P, 8.57; S, 17.75; found C, 49.58; H, 3.29; N, 11.54; P, 8.55; S, 17.63.
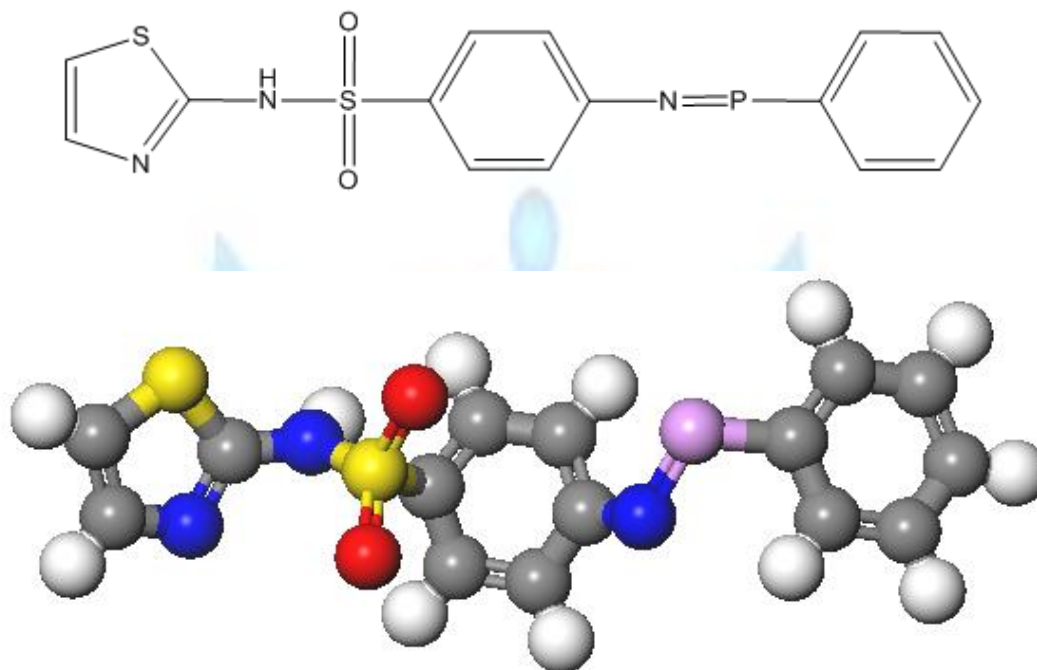

Fig. 1. Proposed structure of HL ligand.

Isolation of complexes

Metal(II)[Co, Ni, Cu, Zn and Hf] chlorides (0.1 mol) was dissolved in ~40 ml absolute ethanol, then added to 0.2 mol of the prepared ligand phenylphosphinylideneamino-N-thiazolyl benzene-sulfonamide (HL) dissolved in ~40 ml absolute ethanol. The mixture was heated under reflux for ~2 h. The precipitate was filtered off and finally washed with hot ethanol several times.

Analytical data

Complex 1: [$CoC_{30}H_{24}Cl_2N_6O_4P_2S_4$]: Yield-55%, dark blue, m.p. > 300ºC, **Calc**. C, 42.26; H, 2.84; Cl, 8.32; Co, 6.91; N, 9.86; P, 7.27; S, 15.04; **Found** C, 42.21; H, 2.82; Cl, 8.24; Co, 6.90; N, 9.84; P, 7.25; S, 15.00; ^M = 2.28, μ_{eff} = 5.32 B.M.

Complex 2: [$NiC_{30}H_{24}Cl_2N_6O_4P_2S_4$]: Yield-54%, dark green, m.p. > 300ºC, **Calc**. C, 42.27; H, 2.84; Cl, 8.32; N, 9.86; Ni, 6.89; **Found** C, 42.14; H, 2.78; Cl, 8.18; Co, 6.89; N, 9.76; P, 7.20; S, 14.93; ^M = 4.86, μ_{eff} = 3.24 B.M.

Complex 3: [$CuC_{30}H_{24}Cl_2N_6O_4P_2S_4$]: Yield-58%, dark brown, m.p. > 300ºC, **Calc**. C, 42.03; H, 2.82; Cl, 8.27; Cu, 7.41; N, 9.80; P, 7.23; S, 14.96; **Found** C, 41.93; H, 2.78; Cl, 8.22; Cu, 7.34; N, 9.75; P, 7.25; S, 14.87; ^M = 2.89, μ_{eff} = 2.12 B.M.

Complex 4: [$ZnC_{30}H_{24}Cl_2N_6O_4P_2S_4$]: Yield-50%, yellow, m.p. > 300ºC, **Calc**. C, 41.94; H, 2.82; Cl, 8.25; N, 9.78; P, 7.21; S, 14.93; Zn, 7.61; **Found** C, 41.87; H, 2.76; Cl, 8.19; N, 9.72; P, 7.17; S, 14.68; Zn, 7.58; ^M = 2.89, μ_{eff} = diamagnetic.

Complex 5: [$HfC_{30}H_{24}Cl_2N_6O_4P_2S_4$]: Yield-52%, yellow, m.p. > 300ºC, **Calc**. C, 37.06; H, 2.49; Cl, 7.29; Hf, 18.36; N, 8.64; P, 6.37; S, 13.19; **Found** C, 36.96; H, 2.41; Cl, 7.24; Hf, 18.35; N, 8.58; P, 6.35; S, 13.14; ^M = 2.89, μ_{eff} = diamagnetic.

Oxidation reactions

The aerobic oxidation reactions were carried out in a 25 ml flask at room temperature and at 70 ºC under atmospheric pressure conditions. 0.05 g of the catalyst ([Co(L)$_2$(Cl)$_2$]], [Ni(L)$_2$(Cl)$_2$],[Cu(L)$_2$(Cl)$_2$], [Zn(L)$_2$(Cl)$_2$] or [Hf(L)$_2$(Cl)$_2$]) was taken in 10 ml of acetonitrile. To this, 10 mmol of the oxidant, 30% H$_2$O$_2$ solution and 5 mmol of cyclohexane were added successively and the reaction solution was magnetically stirred for 8 and 12 h. Aliquots of the reaction mixture were taken separately at 8 h and 12 h for product analysis. The blank experiments were also run individually without catalyst and oxidant by following the same reaction procedure. All samples were analysed by Hewlett–Packard gas chromatography (HP 6890) having FID detector, a capillary column (HP-5), with a programmed oven temperature from 50 to 200 ºC and a 0.5 cm^3 min^{-1} flow rate of N$_2$ as a carrier gas. The conversion of cyclohexane and selectivity for cyclohexanol and/or cyclohexanone was calculated as follows:

Conversion % of cyclohexane = 100 × [Initial % –Final %]/Initial %

Selectivity (100) × [GC Peak area % of cyclohexanol and/or cyclohexanone]

×ΣPeak area of total products

3.   Results and discussion

The ligand

HL ligand is formed via the condensation of the sulfa drug under study with dichlorophenylphosphine. It is characterized based on elemental analyses (C, H, N, S and P). The results obtained are in good agreement with those calculated for the suggested formula (Fig. 1).

The ^{1}H NMR spectra of the ligand HL revealed its formation by the presence of–NH– proton signal at δ = 11.1 (brs, ^{1}H, –SO$_2$–NH, exchangeable with D$_2$O). This is further supported by the appearance of stretching vibration band v(–NH–) sulfonamide at 3310 cm^{-1}. Also, the ^{1}H NMR of the ligand exhibits signals at δ (ppm) = 6.5 (d, J = 10.2 Hz, 2H, Ph), 6.64 (d, J = 10.2 Hz, 2H, Ph), 6.8 (d, J = 10.2 Hz, 2H, Ph), 7.5 (d, J = 10.2 Hz, 2H, Ph), 7.8 (d, J = 3.7 Hz, 1H, Ph), 8.0 (t, J = 3.9 Hz, 1H, thiazole-H3) and 8.1 (d, J = 3.9 Hz, 1H, thiazole-H4).

In the ^{13}C NMR spectrum three peaks at 165.9 ppm and 168.3 ppm, 25.6 ppm and 7.7 ppm were observed, being assigned to C=N and C–S respectively. In the ^{31}P NMR spectrum the ^{31}P (C=N) signal is observed at 25.6 ppm.

The mass spectrum of ligand HL showed molecular ion peak at (361, 28%) which corresponding to its molecular formula C$_{15}$H$_{12}$N$_3$O$_2$PS$_2$, base peak at m/z (%) = 99 (100%), peak at 165 (71%), peak at 186 (75%), peak at 297 (3%) which confirms the suggested structure.

Further insight concerning the structure of the ligand is obtained from IR, UV–vis. The IR and UV–vis measurements, of HL ligand will be discussed with its metal complexes.

Metal complexes and characterization

IR spectra and mode of bonding

In the absence of a powerful technique such as X-ray crystallography, IR spectra have proven to be the most suitable technique to give enough information's to elucidate the nature of bonding of the ligand to the metal ion. The IR spectra of the free ligand and metal complexes were carried out in the range 4000–400 cm^{-1}.

The v(C=N) of the thiazole ring occurs at 1620 cm^{-1} after complexation indicating the coordination of the thiazole nitrogen to metal ions [15]. In addition, the ligand exhibits two bands at 1314 and 1166 cm^{-1} due to v_{asym}(SO$_2$) and $v$sym(SO$_2$) stretching vibrations, respectively. Also, it has a band at 3412 cm^{-1} which attributed to v(NH). The bands due to asymmetric and symmetric SO$_2$ group are shifted to lower frequencies upon complexation. While the v(NH) is disappeared or hidden under the broad bands at 3450–3300 cm^{-1} in the spectra of the complexes as the result of the presence of coordinated molecules which is turns make it difficult to confirm the enolization of the sulfonamide group. In the far IR spectra of all the complexes, the non-ligand bands observed at 500–503, 455–459 and 412–415cm^{-1} regions can be assigned to v(M–O), v(M–N) and v(M–Cl), respectively [16].

From the infrared spectra, it is apparent that, the chelation of the divalent metal ions to the ligand occurs from the HL ligand through the oxygen atom of the sulfonamide group and the nitrogen atom of the thiazole ring in the ligand.

NMR spectra

Unfortunately, the insolubility of either Zn(II) or Hf(II) complexes in CDCL$_3$, CD$_3$COCD$_3$ or DMSO-d6 make it difficult to carry out ^{1}H NMR, ^{13}C NMR and ^{31}P NMR spectra of the complexes to further clarify the way of binding of HL ligand to the metal ions.

Molar conductance measurements

The observed very low molar conductance of the complex in DMSO (10^{-2}M) solution at room temperature was consistent with non-electrolyte nature of the complexes [17]. Thus the complexes may be formulated as [M(L)$_2$(Cl)$_2$], where M= Co(II), Ni(II), Cu(II), Zn(II) and Hf(II), L = ligand.

Mass spectra

The mass spectrum of the Ni complex showed a molecular ion $[NiC_{30}H_{24}Cl_2N_6NiO_4P_2S_4]^+$ peak at m/z 852.36 amu and Hf(II) complex showed molecular ion peak at m/z 676 amu. The calculated mass of Hf(II) complex was 972.15 amu, therefore, the molecular ion peak may be corresponding to the M+ peak. The observed data were in good agreement with the proposed molecular formula that is [M ($C_{30}H_{24}Cl_2N_6NiO_4P_2S_4$) Cl_2] and suggest the monomeric nature of the complexes. In addition to the molecular ion peaks, the spectra exhibit other peaks assignable to various fragments arising from the thermal cleavage of the complexes.

Electronic and magnetic moment measurements

The Co(II) complex showed the magnetic moment 5.32μB for complex (**4**) at room temperature where that of the usual octahedral complexes are 4.8–5.4 B.M [15, 18]. The electronic spectrum of the Co(II) complex displays three bands at 13,256, 15,856 and 24,477 cm^{-1}. These bands may be assigned to following transitions $^4T_1g \rightarrow {}^4T_2g(F)$ (v_1), $^4T_1g \rightarrow {}^4A_2g(F)$ (v_2) and $^4T_1g \rightarrow {}^4T_1g(P)$ (v_3), respectively. The position of bands suggest octahedral geometry of Co(II) complex [18].

The magnetic moment was measured which gave 3.24μB, for complex (**5**), which lies in the range (2.9–3.3μB) of the Ni(II) octahedral complexes [15, 18]. Electronic spectrum of Ni(II) complex displays bands at 14,439, 15,225 and 21,745 cm^{-1} These bands may be assigned to $^3A_2g(F)\rightarrow{}^3T_2g(F)(v_1)$, $^3A_2g(F)\rightarrow {}^3T_1g(F)(v_2)$ and $^3A_2g(F) \rightarrow{}^3T_1g(P)(v_3)$ transitions, respectively. It suggests octahedral geometry of Ni(II) complex [15, 18].

The observed magnetic moment of the Cu(II) complex is 2.21 B.M., which confirms the octahedral structure of this complex [15, 18]. For octahedral Cu(II) complex, the expected transition is $^2B_1g\rightarrow{}^2A_1g$ with respective absorption at 15,398 cm^{-1}. Due to Jahn–Teller distortions, Cu(II) complexes give a broad absorption between 600 and 700 nm.

Ligand field parameters

Various ligand field parameters are calculated for the complexes (Table 1). The value of Dq in Co(II) complexes were calculated from transition energy ratio diagram using the u_3/u_2 ratio [18]. The nephelauxetic parameter β was readily obtained by using the relation β =B (complex)/B (free ion), where B (free ion) for Ni(II) is 1042 cm^{-1} and for Co(II) is 1117 cm^{-1} [18]. The value of β lies in the range 0.47–0.95. These values indicate the appreciable covalent character of metal ligand σ bond. The g values are almost equal to free electron g value.

Table 1: Ligand field parameters of the complexes

Complex	Ligand field parameters				
	Dq (cm^{-1})	B(cm^{-1})	β	g	LFSE (kJ mol−1)
[Co(BHBDAB)(H$_2$O)$_2$]2H$_2$O	422	683	0.47	2.98	48
[Ni(BHBDAB)(H$_2$O)$_2$]2H$_2$O	969	1042	0.95		148
[Cu(BHBDAB)(H$_2$O)$_2$]2H$_2$O	–	–	–	2.10	–

EPR spectrum of Cu(II) complex

The spectrum of the Cu(II) complex exhibits two broad band with $g// = 2.18$ and $g\perp$ 2.06 so, $g// > g\perp > 2.0023$, indicating that the unpaired electron of Cu(II) ion is localized in the $dx^2 –y^2$ orbital. In axial symmetry, the g values are related to the G-factor by the expression G = $(g||–2)/ (g\perp–2) = 4$. The G values of the Cu(II) complex are < 4 suggesting that the considerable exchange interaction in the solid state. Further, the shape of the ESR spectrum of Cu(II) complex indicates that the geometry around the Cu(II) ions are elongated octahedron. The lower value of α^2 (0.46) compared to β^2 (1.04) in Cu(II) complex indicate that the covalent in-plane σ-bonding is more pronounced than the covalent in-plane π-bonding character [18].

Kinetics of thermal decomposition

In order to characterize the metal complexes more fully in terms of thermal stability, their thermal behaviors were studied. In the present investigation, the correlations between the different decomposition steps of the complexes with the corresponding weight losses are discussed in terms of the proposed formula of the complexes. The weight losses for each complex are calculated within the corresponding temperature ranges.

The [Hf(L)$_2$(Cl)$_2$] complex with the molecular formula [Hf $C_{30}H_{24}Cl_2HfN_6O_4P_2S_4$] is thermally decomposed in four successive steps. The first estimated mass loss 24.42% (calculated mass loss = 25%) within the temperature range 58–186 ºC can be attributed to the loss of ($C_{12}H_{10}P_2N_2$) fragment. The DTG curve gives an exothermic peak at 214 ºC (the maximum peak temperature). The second estimated mass loss of 15.39% (calculated mass loss = 15.63%) within the temperature range 186–324 ºC could be attributed to the liberation of ($C_{12}H_8$) fragment. The DTG curve gives an exothermic peak at 333 ºC (the maximum peak temperature). The third estimated mass loss 38.98% (calculated mass

loss = 39.22%) within the temperature range 324–589 ºC can be attributed to the loss of ($C_6H_6N_4S_4O_3Cl_2$) fragment. The DTG curve gives an exothermic peak at 563 ºC (the maximum peak temperature). The fourth step occurs within the temperature range 589–798 ºC with an estimated mass loss 19.94% (calculated mass loss = 19.95%), which is reasonably accounted for the loss of rest of the ligand molecule ($C_{11}H_{13}N_2$), leaving HfO as residue with total estimated mass loss of 78.52% (calculated mass loss = 79.86%). The DTG curve gives an exothermic peak at 675 ºC (the maximum peak temperature).

The thermodynamic activation parameters (Table 2) of decomposition processes of the metal (Co(II), Ni(II), Cu(II) and Zn(II)) complexes namely activation energy (E^*), entropy (ΔS^*) and Gibbs free energy change of the decomposition (ΔG^*) were evaluated graphically by employing three methods, Coats–Redfern [19] (CR), Horowitz–Metzger [20] (HM), and Piloyan–Novikova [21] (PN). From the results obtained, the following remarks can be pointed out:

(1) The high values of the energy of activation, Ea of the complexes reveal the high stability of such chelates due to their covalent bond character [22].

(2) The positive sign of ΔG for the investigated complexes reveals that the free energy of the final residue is higher than that of the initial compound, and all the decomposition steps are non spontaneous processes. Also, the values of the activation, ΔG increases significantly for the subsequent decomposition stages of a given complex. This is due to increasing the values of TΔS significantly from one step to another which overrides the values of ΔH [23].

(3) The negative ΔS values for the decomposition steps indicate that all studied complexes are more ordered in their activated states [24].

Table 2

Kinetic parameters of [Cu(BHBDAB)(H₂O)₂]2H₂O:

Compound	Stage	TG range (°C)	DTG A peak (°C)	A (S^{-1})	E_a (kJ/mol)	ΔH^* (kJ/mol)	ΔS^* (kJ/mol K)	ΔG^* (kJ/mol)
Using Coast–Redfern equation								
[Hf(L)₂(Cl)₂]	1st	58–186	214	46.34×10^6	133.45	125.33	−0.009	125
	2nd	186–324	333	78.87×10^8	142.78	132.12	−0.025	144
	3rd	324–589	5636	77.22×10^{10}	154.68	158.54	−0.034	169
	4th	589–798	75	45.92×10^{13}	164.68	174.56	-0.048	224
Using Horowitz–Metzger equation								
[Hf(L)₂(Cl)₂]	1st	58–186	214	46.34×10^6	134.48	124.34	−0.005	126
	2nd	186–324	333	78.87×10^8	147.18	132.08	−0.024	147
	3rd	324–589	563	77.22×10^{10}	155.84	156.42	−0.038	169
	4th	589–798	675	45.92×10^{13}	168.79	173.33	-0.044	228
Using Piloyan–Novikova equation								
[Hf(L)₂(Cl)₂]	1st	58–186	214	45.66×10^5	134.33	123.43	−0.007	129
	2nd	186–324	333	23.78×10^7	147.34	136.09	−0.024	143
	3rd	324–589	563	45.47×10^9	155.78	152.46	−0.034	162
	4th	589–798	675	47.89×10^{11}	168.64	172.29	-0.043	244

Powder XRD

Single crystals of the complexes could not be prepared to get the XRD and hence the powder diffraction data were obtained for structural characterization. Structure determination by X-ray powder diffraction data has gone through a recent surge since it has become important to get to the structural information of materials, which do not yield good quality single crystals. The indexing procedures were performed using (CCP4, UK) CRYSFIRE program [18] giving tetragonal crystal system for [Co(L)$_2$(Cl)$_2$] having M(9) = 11, F(6) = 8, cubic crystal system for [Ni(L)$_2$(Cl)$_2$] having M(6) = 13, F(6) = 7 and tetragonal crystal system for [Cu(L)$_2$(Cl)$_2$] having M(6) = 19, F(6) = 8, as the best solutions. Their cell parameters are shown in Table 3.

Table 3. Crystallographic data for the Schiff base complexes [Cu(L)$_2$(Cl)$_2$], [Ni(L)$_2$(Cl)$_2$] and [Co(L)$_2$(Cl)$_2$].

Data	[Cu(L)$_2$(Cl)$_2$]	[Ni(L)$_2$(Cl)$_2$]	[Co(L)$_2$(Cl)$_2$]
Empirical formula	CuC$_{30}$H$_{24}$Cl$_2$N$_6$O$_4$P$_2$S$_4$	NiC$_{30}$H$_{24}$Cl$_2$N$_6$O$_4$P$_2$S$_4$	CoC$_{30}$H$_{24}$Cl$_2$N$_6$O$_4$P$_2$S$_4$
Formula weight(g/mol)	857.21	852.36	852.6
Wavelength(Å)	1.49998	1.49998	1.51993
Crystal system	Tetragonal	Cubic	Triclinic
Space group	P4/m	P4/m	P4/m
Unit cell dimensions(Å,°)			
a(Å)	8.200358	16.1056	7.301453
b(Å)	8.200417	16.1048	7. 301453
c(°)	16.02308	16.1048	7. 301453
α(°)	90	90	90
β(°)	90	90	90
γ(°)	90	90	90
Volume (Å^3)	1097.63	5168.52	856.46
(Calc.) density (g/cm^{-3})	1.92584	1.28	1.92
2θ range	13.22–56.38	16.18–64.75	12.48–68.08
Limiting indices	0≤h≤3, 0≤k≤1, 1≤l≤7	3≤h≤10, 1≤k≤6, 3≤l≤10	2≤h≤8, 1≤k≤8, 0≤l≤2
Z	2	6	6
Rf	0.0000801	0.000011	0.0000698
Temperature (K)	298	298	298

SEM and EDX spectra

A representative scanning electron microscopy (SEM) and energy dispersive x-ray analysis (EDX) analysis results of the residue obtained from thermal decomposition of all complexes are shown in Fig. 2. They provide insights on the surface morphology and the composition.

The SEM micrographs of ligand and its complexes are shown in Fig. 2a–f. The Co(II) complex shows bar like structure. The Ni(II) complex shows faceted microcrystal. Agglomerated morphology was seen for the Cu(II) complex. For Hf(II) complex bar with layered structure was present. The EDX spectra show that the residues majorly consist of metal (cobalt, nickel and copper) and oxygen with some traces of sulfur.
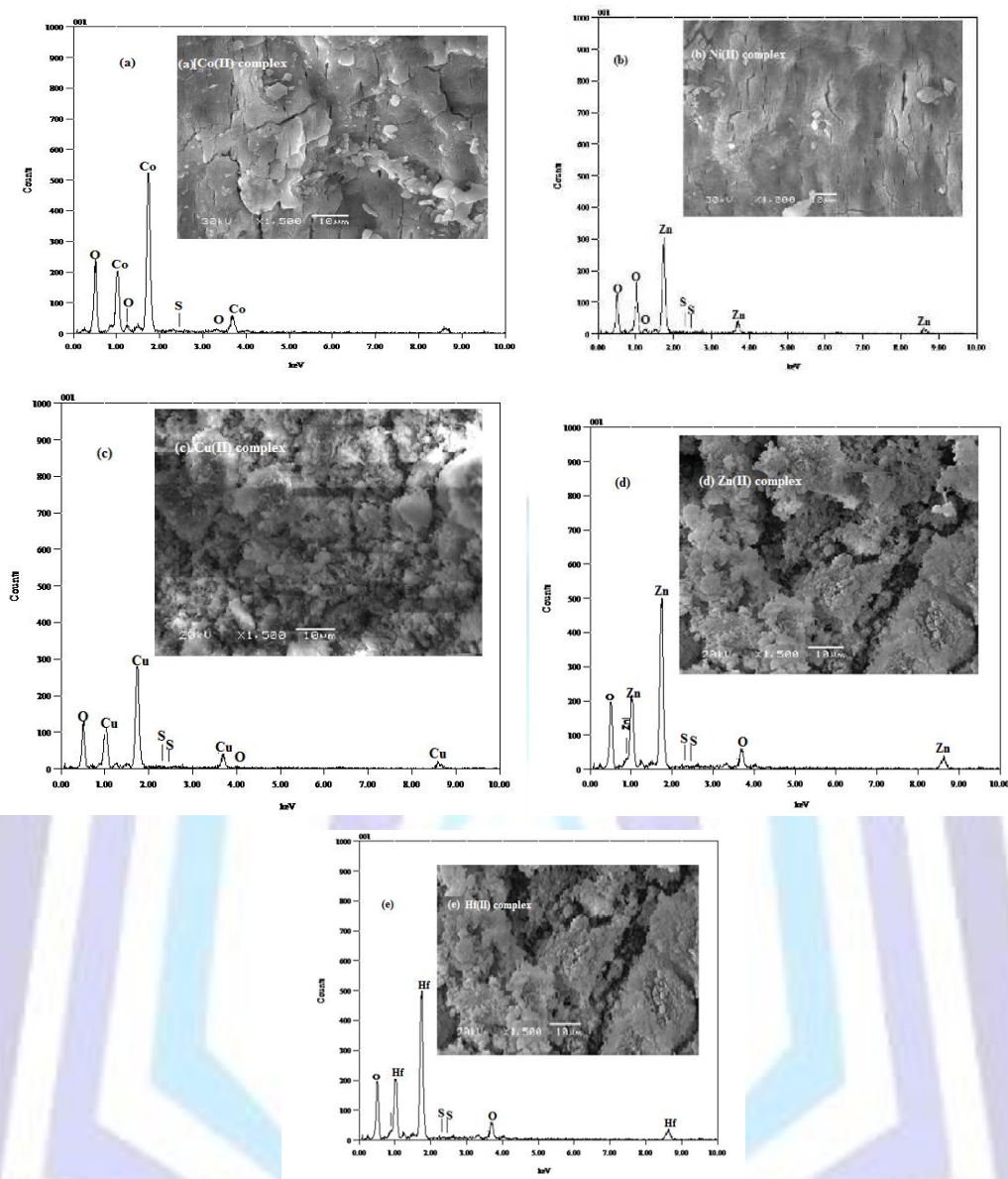
Fig. 2. SEM and EDX spectra for (a) Co(II), (b) Ni(II), (c) Cu(II), (d) Zn(II), and (e) Hf(II) complexes (a-f), respectively.

Cyclic voltammetry

The cyclic voltammogram (Fig.3) of metal(II) complexes were recorded in DMSO at room temperature. The Co(II) and Ni(II) complexes showed well distinguished cathodic peak in the range of -622 mV and the corresponding anodic peak at the range of -947 mV. The measured ΔEp values (ΔEp= - 325) clearly indicated that these redox couples were found to be less stable. The Cu(II) complex also showed redox couples with anodic peak at -668 mV and cathodic peak -497 mV respectively and ΔEp: -188 mV. The ipa/ipc values for complexes cobalt and copper 1.12 and 2.07 respectively, which clearly confirmed the involvement of one and two electron redox process. The measured ΔEp values for these complexes are -325 and -188 mV which clearly indicated that the redox couples are quasi-reversible process.
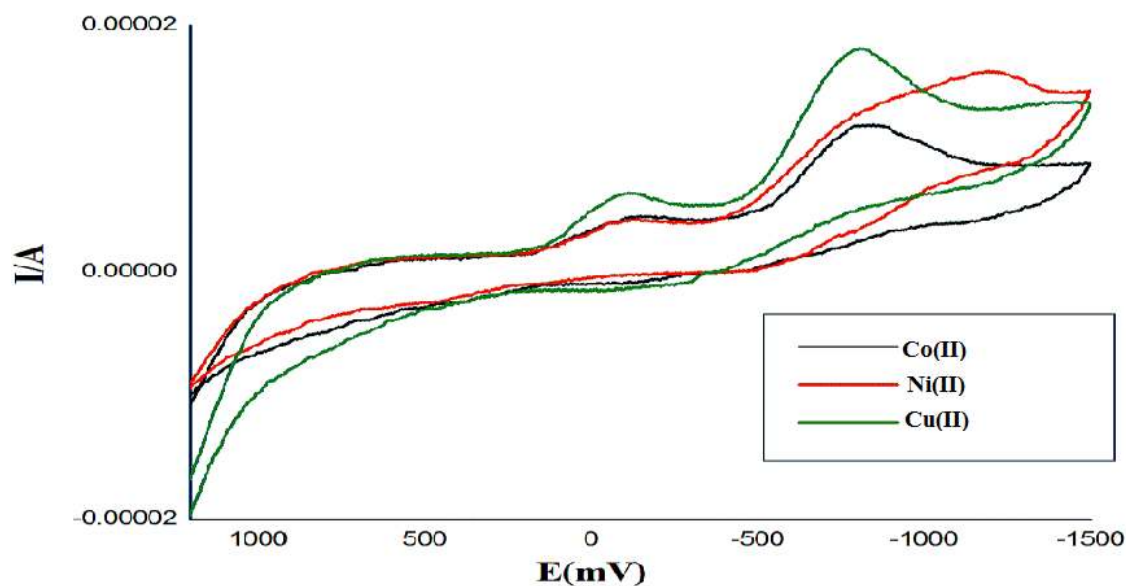
Fig.3. Cyclic voltammograms of Co(II), Ni(II) and Cu(II) complexes.

Catalytic activity

The catalytic activity of cyclohexane oxidation was performed over the five synthesized complexes ([Co(L)$_2$(Cl)$_2$], [Ni(L)$_2$(Cl)$_2$],[Cu(L)$_2$(Cl)$_2$], [Zn(L)$_2$(Cl)$_2$] or [Hf(L)$_2$(Cl)$_2$]) at room temperature (RT) and 70 ºC for 8 and 12 h. The complexes have not showed any conversion of cyclohexane to cyclohexanol and cyclohexanone at RT. Though all synthesized complexes have not yielded any product at RT, cyclohexane conversion can be achieved at particular temperature which is almost close to the boiling point of the reactant. The cyclohexane boiling point is ~79 ºC and thus the reaction temperature fixed at 70 ºC.

Molecular modelling

The ligand–M(II) complexes [M = Co(II), Hf(II)] were modeled by material studio DMOL3 program [25]. Ligand containing metal ion was optimized using molecular mechanic methods. Several cycles of energy minimization had to be carried out for each of the molecules. The root mean square gradient for the molecules was less than one.

The Co(II) complex has octahedral geometry with auto optimized energy 1438.32 kJ/mol. The equatorial positions being occupied by the four N atoms. The equatorial Co(II)-N distance being 1.87 Å. The axial position is occupied by chlorine ligand at Co(II)-Cl distance of 2.37Å. These values are close to the ideal distance of 1.86Åand 2.32 Å, respectively. The N–Co–O and Cl–Co–Cl angles are 86.26Å and 89.75Å, respectively (Fig. 4).

The Hf(II) complex also has octahedral geometry with auto optimized energy 2014.74 kJ/mol. The equatorial Hf(II)-N distance being 1.81 Å. The axial position is occupied by chlorine ligand at Hf(II)-Cl distance of 2.38 Å. These values are close to the ideal distance of 1.86Å and 2.37 Å, respectively. The N–Hf–O and Cl–Hf–Cl angles are 83.17Å and 87.45Å, respectively (Fig. 5).
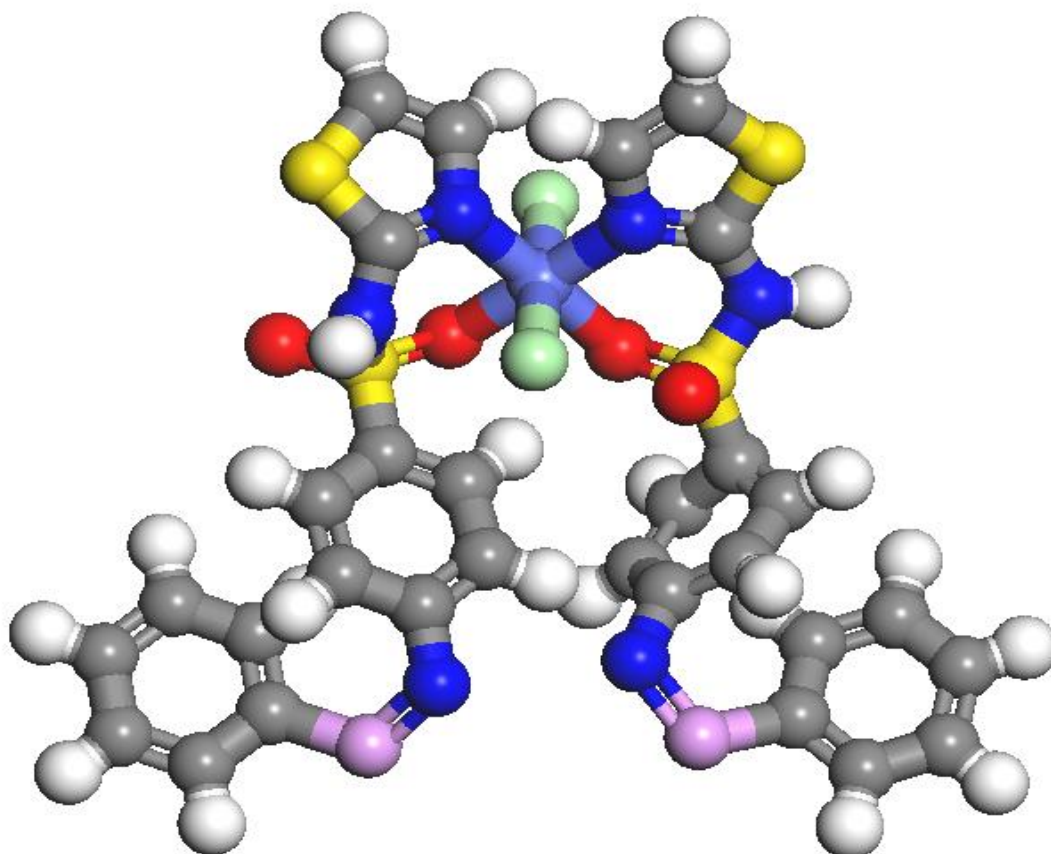
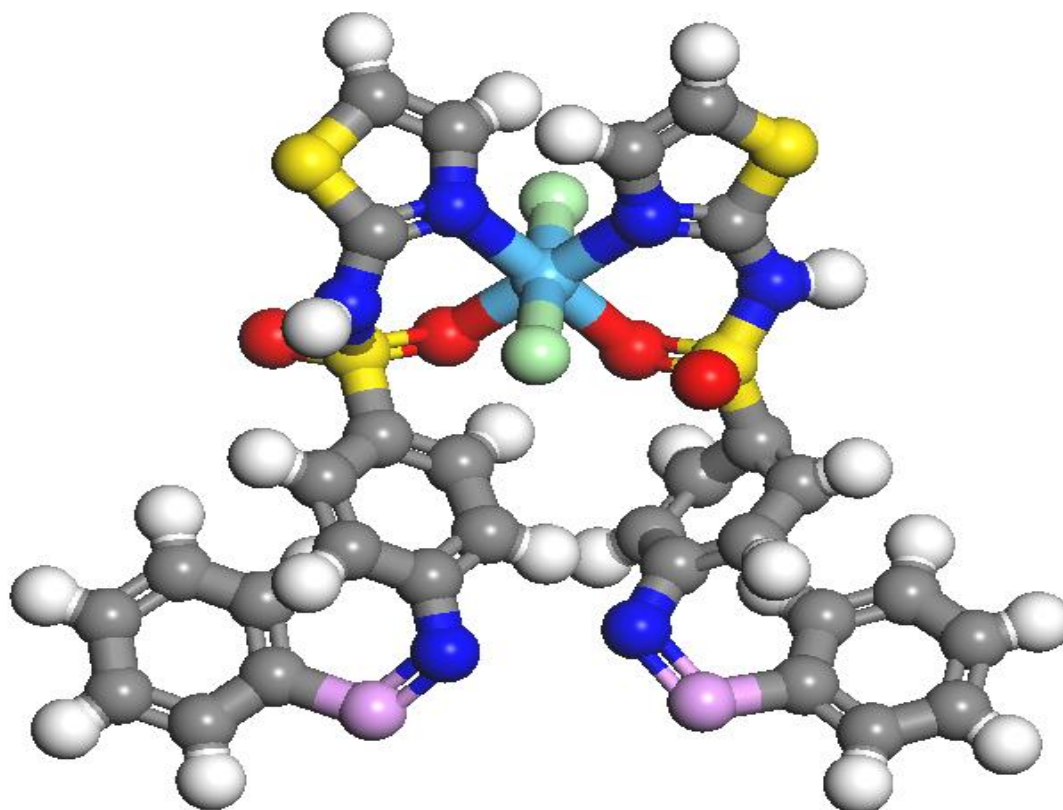**Fig. 4. Geometry optimized structure of [Co(L)$_2$(Cl)$_2$]complex.**

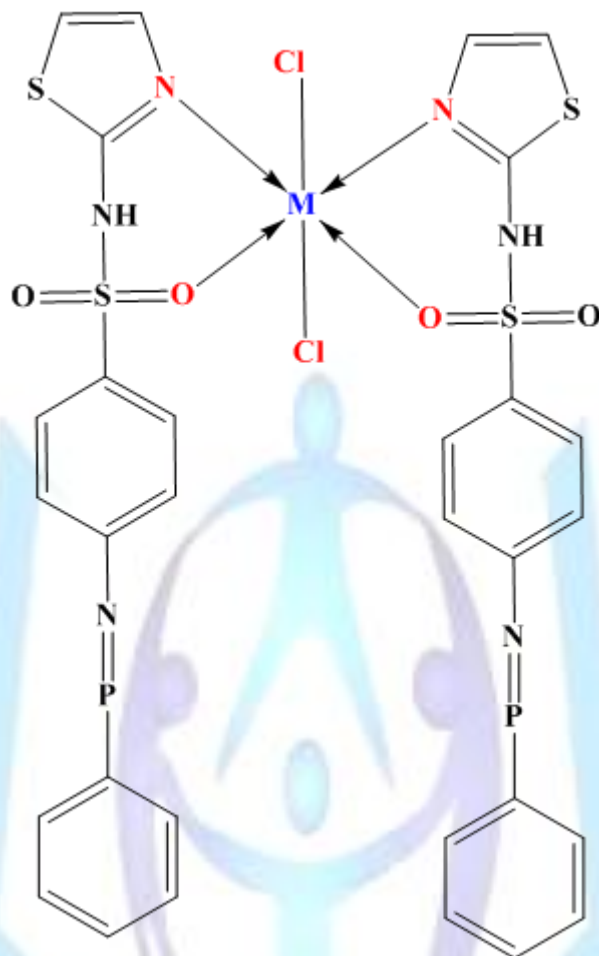**Fig. 5. Geometry optimized structure of [Hf(L)$_2$(Cl)$_2$] complex.**

Finally, the previous findings indicated that the coordination occurs through the nitrogen of the thioazole ring and the oxygen of the sulfonamide –SO$_2$NH– group to give the structures shown in Fig. 6.

M=Cu(II), Co(II), Ni(II), Zn(II) and Hf(II)

Fig. 6. The proposed structures of HL complexes

References

[1] J.J. Pignatello, E. Oliveros, A. MacKay, Crit. Rev. Environ. Sci. Technol. 36 (1) (2006) 1–84.

[2] F. Derek, L. Laine, I.F. Cheng, Microchem. J. 85 (2007) 183–193.

[3] A. Bhunia, S. Durani, P.P. Wangikar, Biotechnol. Bioeng. 72 (5) (2001) 562–567.

[4] L. Levin, L. Papinutti, F. Forchiassin, Biores. Technol. 94 (2) (2004) 169–176.

[5] K. Knutson, S. Kirzan, A. Ragauskas, Biotechnol. Lett. 27 (11) (2005) 753–758.

[6] Q. Husain, Crit. Rev. Biotechnol. 26 (4) (2006) 201–221.

[7] N. Kang, D.S. Lee, J. Yoon, Chemosphere 47 (9) (2002) 915–924.

[8] C.P. Huang, Y.H. Huang, Appl. Catal. A: Gen. 346 (1–2) (2008) 140–148.

[9] C. SJnchez, Biotechnol. Adv. 27 (2) (2009) 185–194.

[10] C. Crestini, R. Saladino, P. Tagliatesta, T. Boschi, Bioorg. Med. Chem. 7 (9) (1999) 1897–1905.

[11] A. Santos, P. Yustos, S. Rodriguez, E. Simon, F. Garcia-Ochoa Jnal, Hazard.Mater. 146 (3) (2007) 595–601.

[12] K. He, Y.M. Dong, Z. Li, L. Yin, A.M. Zhang, Y.C. Zheng Jnal, Hazard. Mater. 159 (2–3) (2008) 587–592.

[13] Kyoung-Hun Kim, Son-Ki Ihm, J. Hazard. Mater. 186 (1) (2011) 16–34.

[14] L.F. Liotta, M. Gruttadauria, G. Di Carlo, G. Perrini, V. Librando, J. Hazard. Mater. 162 (2–3) (2009) 588–606.

[15] C. M. Sharaby, Spectrochimica Acta Part A 66 (2007) 1271–1278.

[16] A. M.A. Alaghaz, . Molecu. Struct. 1068 (2014) 27–42.

[17] W.J. Geary, Coord. Chem. Rev. 7 (1971) 81–122.

[18] M. M. Al-Mogren, A. M.A. Alaghaz, E. A. Ebrahem, Spectrochimica Acta Part A 114 (2013) 695–707.

[19] A.W. Coats, J.P. Redfern, Nature 20 (1964) 68–69.

[20] H.H. Horowitz, G. Metzger, Anal. Chem. 35 (1963) 1464–1468.

[21] G.O. Piloyan, T.D. Pyabonikar, C.S. Novikova, Nature, 212 (1966) 1229–1304.

[22] T. Taakeyama, F.X. Quinn, Thermal Analysis Fundamentals and Applications to Polymer Science, John Wiley and Sons, Chichester, 1994.

[23] P.B. Maravalli, T.R. Goudar, Thermochim. Acta 325 (1999) 35–41.

[24] L.T. Valaev, G.G. Gospodinov, Thermochim. Acta 370 (2001) 15–19.

[25] Materials studio v 5.0, copyright Accelrys software Inc., 2009.

Figure captions

Fig. 1. Proposed structure of HL ligand.

Fig. 2. SEM and EDX spectra for (a) Co(II), (b) Ni(II), (c) Cu(II), (d) Zn(II),   and (e) Hf(II) complexes (a-f), respectively.

Fig.3. Cyclic voltammograms of Co(II), Ni(II) and Cu(II) complexes.

Fig. 4. Geometry optimized structure of $[Co(L)_2(Cl)_2]$complex.

Fig. 5. Geometry optimized structure of $[Hf(L)_2(Cl)_2]$ complex.

Fig. 6. The proposed structures of HL complexes